Thank you for your constructive comments, which were useful to improve our paper. Please see our responses below. The comments are in **bold** *italics* while the responses are in normal type.

Why do you set the maximum lasting hour as 12 hour? It seems to me more reasonable if you don't set this one but only set the precipitation rate since there may be some convection events lasting longer than 12 hours. Have you checked that in the simulation, how much of the convection events lasting longer than 12 hours?

We found that by setting the maximum lasting hour to 12 hours, we captured almost all events in CanAM4.3 and spCAM5. For instance, Figure 1(c) shows that less than 0.1 % of the events in CanAM4.3 last longer than 4.5 hours and less than 1 % of spCAM5 events last longer than 5 hours. Therefore, reducing the threshold to 6 hours or increasing the threshold to 24 hours will not affect the results in this paper.

The following text have been added to Section 4.2 in the manuscript:
"and only 1 % of the events last longer than 5 h"
"and only 0.1 % of the events last longer than 5 h"

Here, you checked the near-surface vertical velocity when considering the relationship between convection and large-scale environment. As shown in Song and Zhang (2017) you cited in the paper, the dCAPELSFT is mainly contributed by the vertical velocity and the vertical structure of large-scale vertical velocity is important for the convection development. Hence, could you also check the vertical structure of vertical velocity here? For example, similar to figure 2, could you also show the convective precipitation as function of different vertical velocity?

Additional Figure 2 (below) shows the convective precipitation as function of dCAPELSFT and vertical velocity at various levels, 232 hPa (top panel), 524 hPa, 763 hPa, 887 hPa, and 992 hPa (bottom panel). spCAM5 is on the left and CanAM4.3 is on the right. Additional Figure 2 shows that convective precipitation in CanAM4.3 has no dependency on omega but convective precipitation in spCAM5 it does depend on omega. In general, heavier precipitation in spCAM5 is linked to more negative (upward advection) omega at 992 hPa and less negative omega at 232 hPa. Since omega was computed from the large-scale horizontal winds starting from the top of the troposphere using the continuity equation, a negative omega at pressure p0 is approximately equal to the net column mass convergence above the level p0. Therefore, high rainfall rates in spCAM5 are associated with strong low-level ascent (net column mass convergence) and larger dCAPELSFT.

In addition Figure 2(a) shows that, when dCAPELSFT is smaller than 50 J kg-1 h-1, convection precipitation is almost independent of near-surface vertical velocity, but when dCAPELSFT becomes larger and larger, the dependence of convective precipitation on the near surface vertical velocity seems much tighter. It is a quite interesting phenomenon, maybe you can dig it further and check whether it is also the case for different levels of vertical velocity.

Indeed this is an interesting phenomenon. The left side panels in Additional Figure 2 (below) show that when dCAPELSFT is less than 50 J kg-1 h-1 convective precipitation

is nearly independent of near-surface omega, as well as omega at other levels. In addition, Figure 2(a) in the manuscript shows that, when dCAPELSFT is less than 50 J kg-1 h-1, precipitation varies between 0 and 1 mm h-1. But also, when the near-surface omega in Figure 2(a) is greater than 80 Pa s-1 (strong subsidence), convective precipitation is also nearly independent of dCAPELSFT and varies between 0 and 1 mm h-1. We can argue that, when one of the variables is in its lowest 25 percentile, convective precipitation in spCAM5 does not exceed 1 mm h-1.

The following text have been added to Section 4.3 in the manuscript:
"In the case when one of the quantities is in its lowest 25 percentile, for instance $dCAPE_{LSFT} < 50$ J kg^{-1} h^{-1} or $\omega > 80$ Pa s^{-1}, precipitation rates do not exceed 1 mm h^{-1}".

From Fig. 3, it seems that even for the dCAPELSFT, it is also not a good trigger for convection, since before and after convection (t=0), it doesn't change much (Fig. 3e). How can you set a threshold of dCAPELSFT to judge when the convection occurs. It is quite difficult. Instead, it seems that when convection happens, the tendency of dCAPELSFT becomes positive (d(dCAPELSFT)/dt). Have you further check the relationship between the convective precipitation and d(dCAPELSFT)/dt?

We thank you for this very useful suggestion. From our results in Figure 3(a), convection is likely triggered once near-surface omega becomes negative, which is about 30 minutes prior to time=0. Prior to time=0, dCAPELSFT is nearly constant and thus cannot be used to detect initiation of convection. We did, as the reviewer suggested, investigate the relationship between d(dCAPELSFT)/dt and the precipitation. In Additional Figure 3 d(dCAPELSFT)/dt is in red and convective precipitation is in black, both computed using the spCAM5 fields from Figure 3(a) in the manuscript. From Additional Figure 3, d(dCAPELSFT)/dt becomes positive about 20 minutes prior to time=0, and reaches its maximum slightly prior to the precipitation maximum. We have not investigated these findings further, and will leave them for future study. One possibility is that the d(dCAPELSFT)/dt trend might be linked to the trend in the near-surface omega in Figure 3(a).

As shown in Song and Zhang (2018), the dCAPE-type triggers are significantly scale dependent. In the higher-resolution models, it doesn't work very well compared to the coarser model resolution, since the relationship between dCAPE and convective precipitation becomes worse when the resolution is increased. Here, the spCAM5 is 4 km and CanAM4 is about 300 km. From figure 2, it seems that the relationship between convective precipitation and dCAPELSFT is much closer in CanAM4. Could you calculate the correlation and make some discussion about this issue. Reference: Song, F. and G. Zhang, 2018: Full Access Understanding and Improving the Scale Dependence of Trigger Functions for Convective Parameterization Using Cloud-Resolving Model Data, Journal of Climate, 7385-7399.

We used all 32 CRM columns to compute an average spCAM5 convective precipitation and compare this "low-resolution" precipitation to CanAM4.3 convective precipitation. We have not investigated the dependence of spCAM5 precipitation to the number of CRM columns used to compute an average convective precipitation, because that is out of the scope of this paper. We did, however, compute the linear Pearson correlation

coefficient between dCAPELSFT and the convective precipitation and we found that the correlation is higher in CanAM4.3 (0.68) than in spCAM5 (0..44).

Finally, in the spCAM5, dCAPELSFT cannot be regarded as pure large-scale forcing, since it is calculated based on 4km dataset (also see the discussion in Song and Zhang 2018). So how the convection happens in this model should be investigated further, since it provide more accurate description of convection. That will provide more information to the community.

DCAPELSFT was computed using the large-scale T and Q fields and the large-scale T and Q spCAM5 tendencies. It is true that the large-scale tendencies include small-scale tendencies due to various processes that occur within the CRM (4-km) columns, but we should clarify that our goal was to try understand the overall effect of these 4-km small-scale tendencies on the convective precipitation in spCAM5. The overall effect of these small scale tendencies are therefore directly comparable with the overall tendencies generated within the Zhang-McFarlane convection scheme employed in CanAM4.3. The manuscript shows the differences between the overall precipitation and large-scale forcing fields between the two models.

We added the following text to Section 4.3 in the manuscript:

“Therefore, a transition from a large-scale subsidence to large-scale ascent may be important in triggering convection. A near-surface omega tendency has been previously used as a trigger in the Donner convection scheme (Donner 1993; Donner et al. 2001; Wilcox and Donner 2007) in a version of the Geophysical Fluid Dynamic Laboratory (GFDL) Atmospheric model, version 3 (AM3) GCM. In their model, convection is triggered when near-surface omega becomes positive and exceeds a specified value and convective inhibition is less than 100 J kg-1.”.

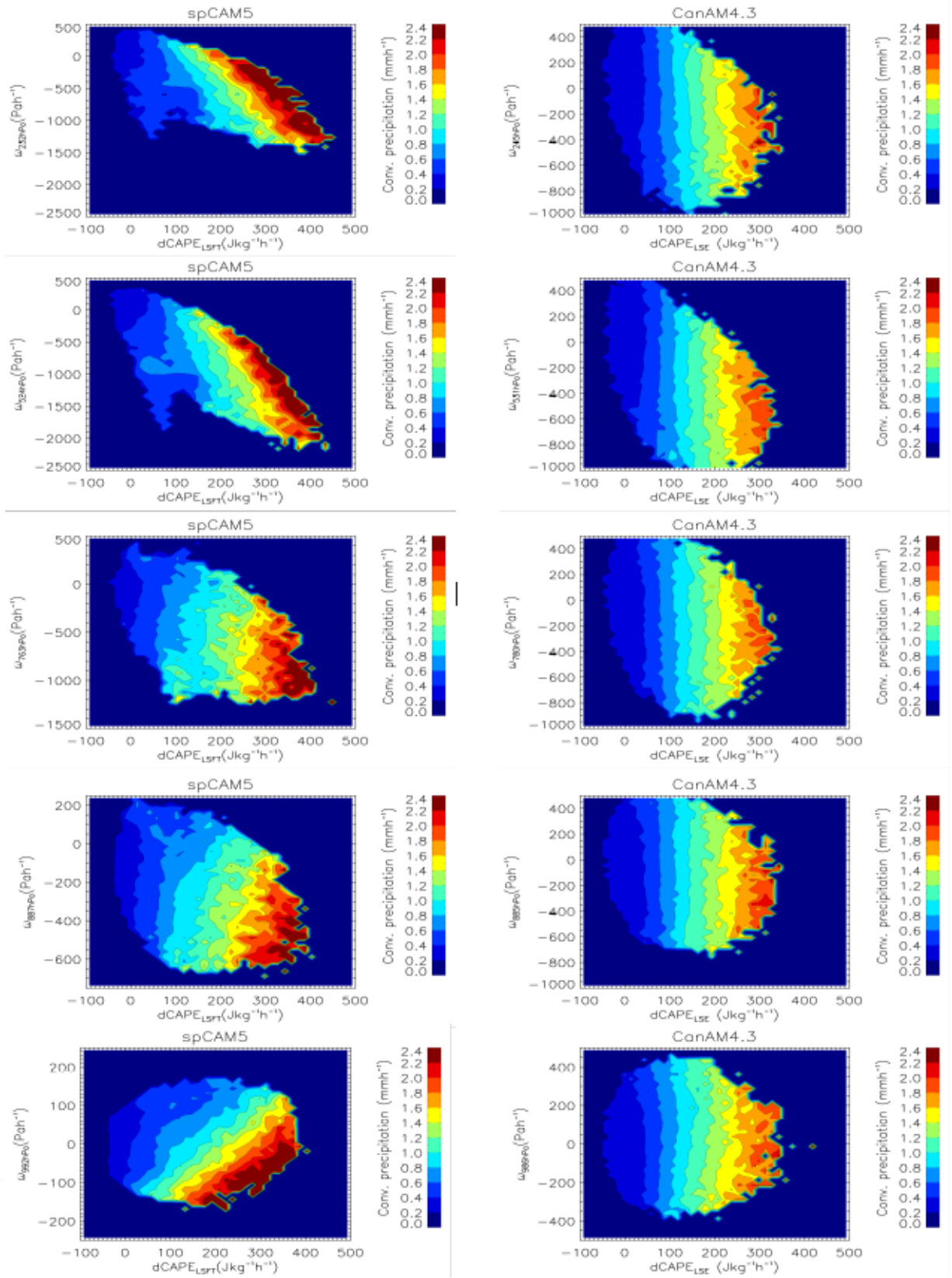

Additional Figure 2

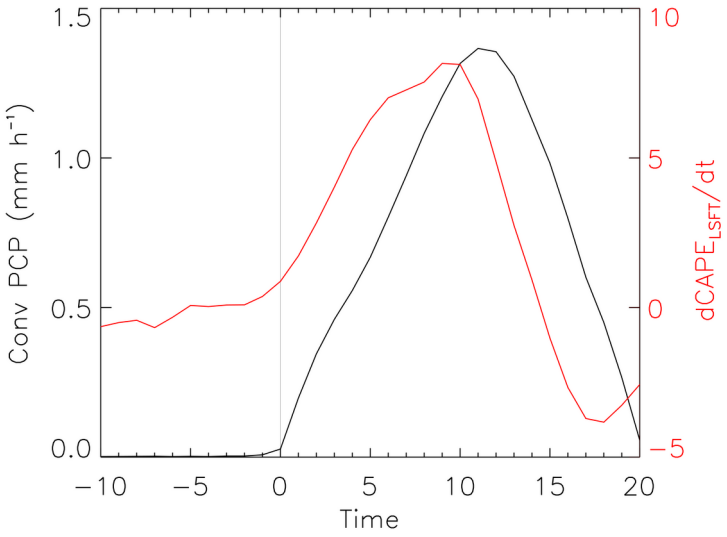

Additional Figure 3

Thank you for your constructive comments, which were useful to improve our paper. Please see our responses below. The comments are in **bold** *italics* while the responses are in normal type.

I encourage the authors to provide a deeper discussion and interpretation of the results. For example, the lack of relationship between convective precipitation and near surface vertical velocity (Figure 2b, 3b) and the mismatch in timing with CAPE/ CIN in CanAM4.3 relative to spCAM5 are particularly interesting findings.

We added the following text in Section 4.4 of the manuscript:

"Therefore, a transition from a large-scale subsidence to large-scale ascent may be important in triggering convection. A near-surface omega tendency has been previously used as a trigger in the Donner convection scheme (Donner 1993; Wilcox and Donner 2007) in a version of the Geophysical Fluid Dynamic Laboratory (GFDL) Atmospheric model, version 3 (AM3) GCM. In their model, convection is triggered when near-surface omega becomes positive and exceeds a specified value and convective inhibition is less than 100 J kg-1".

"Convective precipitation in CanAM4.3 does not seem to correlate well with CIN (Fig. 3b) and this is likely because CIN is not independently included in the ZM closure in CanAM4.3. Therefore, any discussion of CIN and linkage to CanAM4.3 precipitation is out of the scope of this paper. We should point out thought that, CIN is tightly coupled with precipitation over mid-latitude summertime continent but not with precipitation over oceans (Myoung and Nielsen-Gammon, 2010)."

How are the deficiencies in the parameterizations used in CanAM4.3 (i.e., CAPE based closure), which have been identified here, different from what is already known and published?

In the introduction we briefly mentioned that some commonly used convective scheme in GCMs employ triggers and closures based on convective available potential energy (CAPE) or CAPE generation while other closures are based on net column moisture convergence. Other convective schemes, for instance the Donner convective scheme, use grid-scale upward motion in the lower troposphere as trigger function. Although, the Zhang-McFarlane (ZM) convection scheme is very popular and has been modified and improved over time, as described for example in Zhang and Mu, 2005a, the ZM scheme still has deficiencies, such as, generates too frequent too light precipitation and underestimates the frequency of extreme events. However, various models employ various version of the ZM scheme and our goal is not to modify the ZM scheme employed in CanAM4.3, but to compare the precipitation generated within the ZM scheme to precipitation generated within a cloud-resolving model under similar large-scale forcings.

And how can new information from the results presented here be applied to further improve models beyond what has already been implemented?

One new result is that precipitation generated within a cloud-resolving model depends on both CAPE generation and near-surface omega, two commonly used variables in the trigger and closure functions of most popular convective parameterization schemes, while convective precipitation is a function of CAPE only in a CAPE based closure model (CanAM4.3). Another new result is that, the cause-consequence analysis (Figure 3) show that variations in omega precede variations in convective precipitation while variations in CAPE generation trail variations in convective precipitation in spCAM5. Based on these results we suggested that near-surface omega might qualify as better trigger and may be used together with dCAPELSFT in the closure scheme in CanAM4.3.

The effort to calculate "convective precipitation in spCAM5" in a way that is comparable to "convective precipitation in a parameterized model" is a great idea and potentially very useful. However, it is not clear that the way it is calculated in spCAM5 here means the same thing as it does from parameterized convection in CanAM4.3. How sensitive are the results to the values of the criteria (vertical velocity and cloud water/ice)? More importantly, how well does a definition of "convective precipitation " based on CRM vertical velocity and cloud water/ice match what "convective precipitation" means in a global parameterized model? Since the comparison and analysis is contingent on this calculation, it would be useful to discuss other ways it could be defined within spCAM5 and/or expected differences with what convective precipitation means in CanAM4.3. It would also be helpful to use an independent calculation of "convective precipitation" that could be applied identically to both models, which would likely be dependent on large-scale conditions. Ultimately, to what degree do the results and comparison between the models depend on the way that convective precipitation has been defined? Likewise, how is CAPE calculated in spCAM5, is it at the CSRM or GCM scale? A comparison to CAPE calculated at the GCM scale would be most consistent with CAPE from CanAM4.3. Along these same lines, the differences in the relationship of convective precipitation and omega between spCAM5 (strong correlation) and CanAM4.3 (no correlation) may be, in part, due to differences in the definition of convective precipitation. I suggest including some analysis of relationships with "total precipitation rates" or alternative definition of "convective precipitation" in spCAM5.

We agree with the reviewer that the definition of convective precipitation in spCAM5 will be sensitive to the values of the vertical velocity and the cloud water and ice. The method we used to define convective precipitation follows that in Suhas and Zhang (2015) and Song and Zhang (2018). Using this method, 68 % of the total precipitation in spCAM5 was convective compared to 71 % in CanAM4.3.

However, as the reviewer suggested, we further investigated the sensitivity of our results to the definition of convective precipitation. We repeated all the analyses using total precipitation instead of convective precipitation and generated Additional Figure 1, 2(a), 2(c), and 3 (below). The results in the Additional Figures are similar to those in Figure 1, 2(a), 2(c), and 3 in the manuscript. Therefore, we can say that the findings in the manuscript are not sensitive on the details of how the rainfall is partitioned in both spCAM5 and CanAM4.3.

We added the following text in Section 3.1 of the manuscript:

"The sensitivity of the results to the definition of convective precipitation from spCAM5 was evaluated by repeating the analyses using total instead of convective precipitation. The results in Figure 1, 2(a), 2(c), and 3 were found to be similar using either the total or convective precipitation from spCAM5, implying insensitivity, for this study, to the exact definition of thresholds in the method of Suhas and Zhang (2015)."

In general, an explicit inclusion of observations for comparison would be helpful to the reader. The authors note that there is no dependence of convective precipitation with CAPE in spCAM5, which they say is consistent with observations by citing Mitovski and Folkins [2014]. It would be useful to make this calculation and include the observations in the figure for both CAPE and dCAPE. Likewise, the authors note that spCAM5's relationship between min/max CAPE and the timing of rainfall is consistent with observations by referring to Mitovski and Folkins [2014], but again I think showing the actual observations (as referenced) on the same figure would help.

Mitovski and Folkins 2014 used 12-hour vertical profiles of temperature and specific humidity to compute CAPE. In addition, they used 3-hour TRMM 3B42 rainfall to isolate rainfall events. In this paper, however, we use sub-hourly model data to compute CAPE and investigate the relation with convective precipitation. Although the temporal resolution of the data used in Mitovski and Folkins (2014) and in this paper is different, it has been previously shown that tropical convection exhibits similar behavior on various time-scales (Mapes et al., 2006: "The mesoscale convection life cycle: Building block or prototype for large-scale tropical waves?"). The similarity in the observed and simulated (spCAM5) CAPE variation, once again shows that, in absence of higher-resolution observations, spCAM5 may be useful in studying convection-large-scale environment interactions.

To make it clear that Mitovski and Folkins 2014 use 12-hour soundings, we added the following text in Section 4.4 of the manuscript:

"12-hourly"

Minor Comments:

Why not evaluate the ZM scheme as implemented in the conventional CAM5 to have more consistency with spCAM5? Many other aspects of the model are different between CanAM4.3 and spCAM5, beyond just the representation of convection, which makes the comparison somewhat unconstrained. I suggest including results from CAM5 as well as CanAM4.3 and spCAM5. Since only 3 months of simulation time is being assessed here and the initial setup of CAM5 would be the same as sp-CAM5, this should not add a significant amount of work.

We agree that it would be interesting and useful to perform the analysis using CAM5 simulations that are configured the same as spCAM5. However, this is a non-trivial amount of work due since the spCAM5 data we used was archived from previous simulations and we no longer have access to the personnel and computer accounts. To perform the CAM5 would require significant effort to set as it would require setting up the model on a new computer system with all of the associated effort to verify it is

implemented correctly. Repeating the analysis with CAM5, and potentially other model, would be something that could performed in future studies.

I am confused about the vertical resolution used in spCAM5. Typically, the vertical resolution is 30 levels in the global grid and 28 levels in the CSRM (coinciding with the lowest 28 levels). Here the authors state that there are 66 levels CAM5, which would imply 38 levels above the CSRM rather than the typical 2 levels. Have previous studies used this configuration? Have you evaluated the differences between using 30 and 66 levels Additionally, the Khairoutdinov and Randall (2001 and 2003) references are fairly old and refer to the implementation of super-parameterization in older versions of CAM. I recommend the authors cite more recent papers describing the implementation in CAM5, such as Wang et al., 2011 (https://www.geosci-model-dev.net/4/137/2011/gmd-4-137-2011.pdf).

We stated all CAM5 and CanAM4.3 levels in the atmosphere. As the reviewer suggester, we updated the manuscript and include the lower atmosphere levels only, as well as, we cite Wang et al., 2011. We substituted the following text in Section 2:

“66 vertical levels from the surface to 5.1 x 10e-6 hPa “

With:

“30 vertical levels from the surface to 3.6 hPa”

Since spCAM5 is used instead of spCAM4, it includes aerosol processes and two-moment microphysics, so it might be helpful to describe these components of the model (MAM3 aerosol and Morrison microphysics) and compare them with the same processes in CanAM4. The representation of aerosol and cloud microphysics are likely to influence precipitation as well.

We agree that it is possible that the aerosol and cloud microphysics formulation could influence the precipitation but our hypothesis is that the main control in the Tropical Western Pacific is rainfall from the deep convective scheme. In the paper we note that roughly 70% of the rain is convective and it seems that the stratiform rain has little effect on the results (performing the analysis using the total rain or the convective rain give similar results). We leave it to the interested reader to refer to the references for details about the aerosol and cloud microphysics parameterizations.

For the relationship between vertical velocity and convective precipitation in CanAM4.3 (Figure 1a), the authors conclude that "the results are not considered robust due to the few samples". Why not use more years for the CanAM4.3 results? CanAM4.3 is relatively cheap to run, so it is unnecessary for the authors to limit their analysis to such a short period. I recommend using more data, at least for CanAM4.3, to produce more robust results

We found this suggestion very useful and we therefore perform another five CanAM4.3 ensemble simulations for the period of study. The ensemble was generated by changing the random number seed on 1 January 1997. We incorporated the data from these simulations into our analysis. Figures 1, 2, and 3, are now based on 5 CanAM4.3 ensemble runs.

We added the following text in Section 2 of the manuscript:
“For CanAM4.3, a six member ensemble was generated by uniquely adjusting the seed for the random number generator on 1 January 1997. This was done to improve the statistical representation of the results from this model as data from all ensemble members were used in the analysis’.

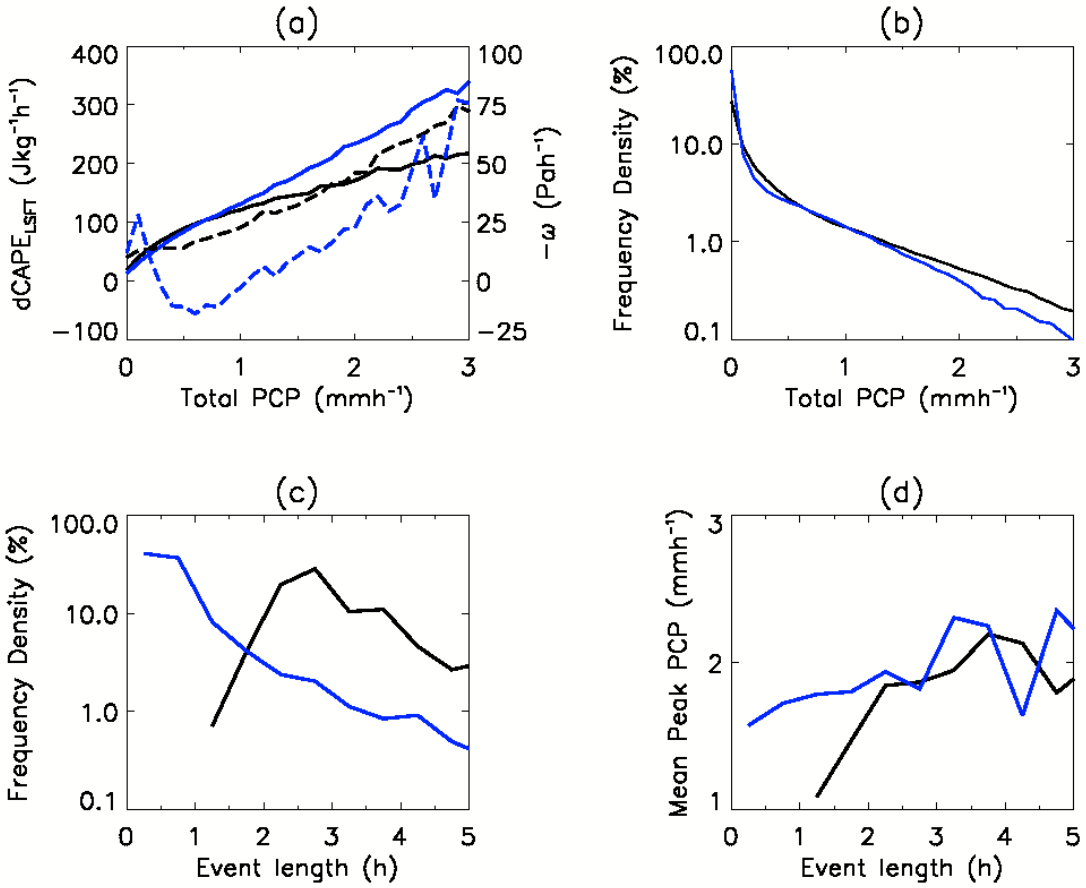

Additional Figure 1

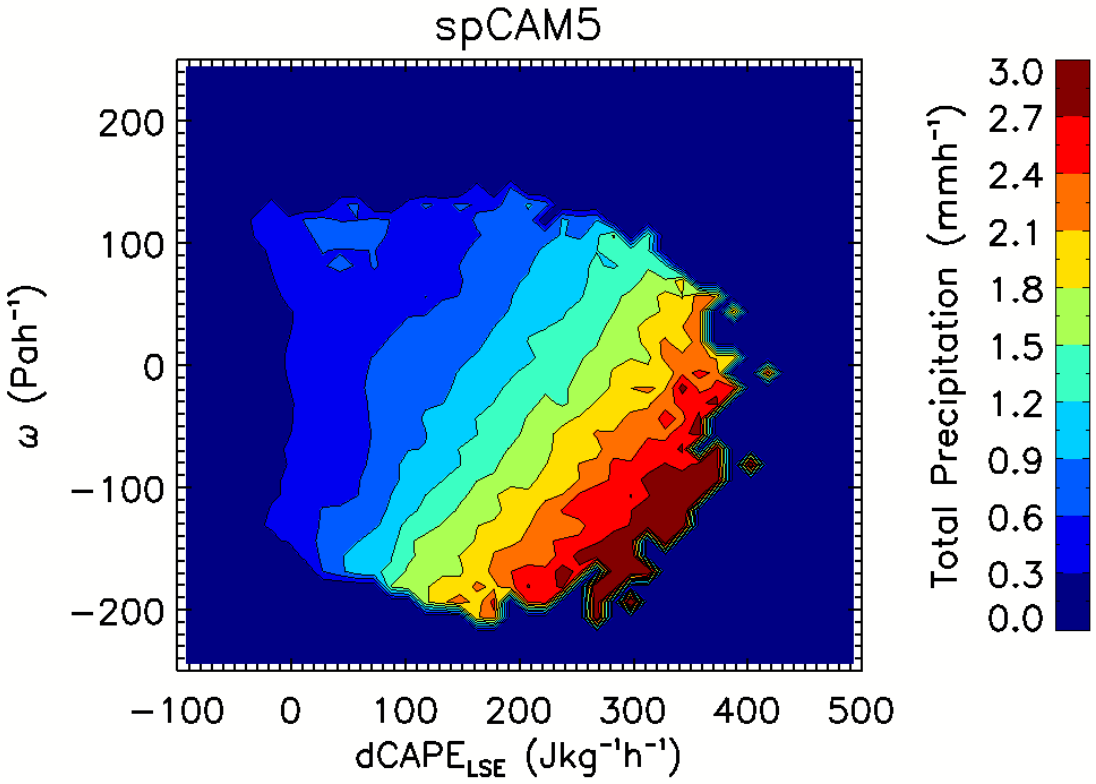

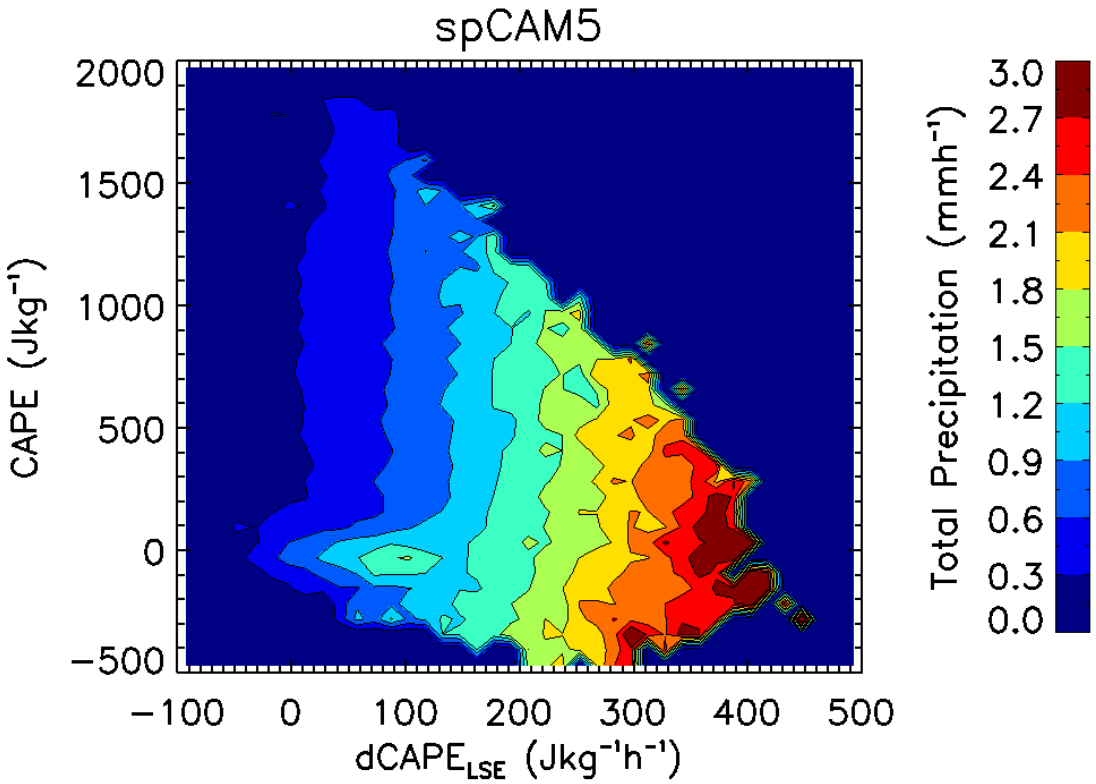

Additional Figure 2(a) and 2(c)

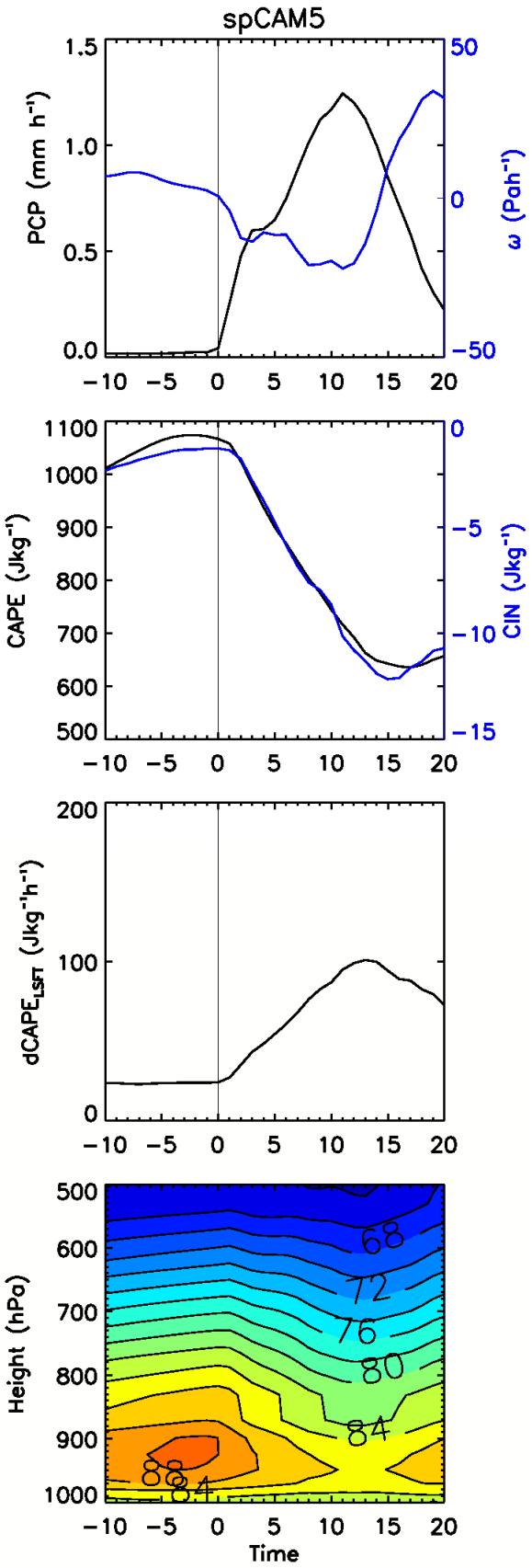

Additional Figure 3

Convective response to large-scale forcing in the Tropical Western Pacific simulated by spCAM5 and CanAM4.3

Toni Mitovski[1], Jason N. S. Cole[1], Norman A. McFarlane[2], Knut von Salzen[2], Guang J. Zhang[3]

[1]Canadian Centre for Climate Modelling and Analysis, Environment Canada, Toronto, ON, Canada
[2]Canadian Centre for Climate Modelling and Analysis, Environment Canada, Victoria, BC, Canada
[3]Scripps Institution of Oceanography, University of California, San Diego, CA, USA

Correspondence to: Jason N. S. Cole (jason.cole@canada.ca)

Abstract. Changes in the large-scale environment during convective precipitation events in the Tropical Western Pacific simulated by version 4.3 of the Canadian Atmospheric Model (CanAM4.3) is compared against those simulated by version 5.0 of the super parameterized Community Atmosphere Model *(*spCAM5). This is done by compositing sub-hourly output of convective rainfall, convective available potential energy (CAPE), CAPE generation due to large-scale forcing in the free troposphere ($dCAPE_{LSFT}$), and near surface vertical velocity (ω) over the time period May-July 1997. Compared to spCAM5, CanAM4.3 tends to produce more frequent light convective precipitation (< 0.2 mm h^{-1}) and underestimates the frequency of extreme convective precipitation (> 2 mm h^{-1}). In spCAM5 5 % of convective precipitation events lasted less than 1.5 h and 75 % lasted between 1.5 and 3.0 h while in CanAM4.3 80 % of the events lasted less than 1.5 h. Convective precipitation in spCAM5 is found to be a function of $dCAPE_{LSFT}$ and the large-scale near surface ω with variations in ω slightly leading variations in convective precipitation. Convective precipitation in CanAM4.3 does not have the same dependency and instead is found to be a function of CAPE.

1 Introduction

Global climate models (GCMs) typically have a horizontal grid-scale that is much larger than individual deep convective clouds which requires parameterizations of convection and its effect on the large-scale atmosphere. Convective and other GCM parameterization often have adjustable parameters “tuned” within their range of uncertainty so that the model simulates reasonable climatological distributions of temperature, clouds, and wind fields (Mauritsen et al., 2012). However, these long-term climatological averages are the result of many shorter time-scale subgrid convective events which may have their biases masked by averaging. It is known that climate models tend to exhibit less rainfall variance than observations (Scinocca and McFarlane, 2004; DeMott et al., 2007), tend to produce light precipitation (< 10 mm day^{-1}) more often than observed (Zhang and Mu, 2005b; Sun et al., 2006; Dai, 2006) and underestimate the occurrence of extreme precipitation events (Wilcox and Donner, 2007; Boyle and Klein, 2010; Wang et al., 2017).

Studies have attributed biases in simulated precipitation variability to convective parameterizations employed in models (Zhang and Mu, 2005b; DeMott et al., 2007; Wang and Zhang, 2013; Wang et al., 2016). In general, convective parameterizations require a closure, which may or may not be activated (triggered) based on whether certain conditions are satisfied. If activated, the closure computes the cloud base mass flux which in turn is used to compute fluxes of mass, moisture, and precipitation above cloud base. Although convective precipitation is generated in response to the closure, it has been shown that the design of the trigger function may also influence the simulation of precipitation (Truong et al., 2009). Commonly used convective schemes employ triggers and closures based on net column moisture convergence

(Tiedtke, 1989) or convective available potential energy (Zhang and McFarlane, 1995) while some convective schemes use grid-scale upward motion in the lower troposphere as a trigger function (Donner, 1993; Bechtold et al., 2001).

A super-parameterization framework (Grabowski, 2001; Khairoutdinov and Randall, 2001) has been used to replace conventional convective and boundary layer parameterizations with cloud system resolving models (CSRMs) in GCMs. When evaluated against observations and compared to GCMs, super-parameterized GCMs show improved tropical rainfall variability associated with the El Niño Southern Oscillation (Stan et al., 2010), the Madden-Julian Oscillation (Thayer-Calder and Randall, 2009; Kooperman et al., 2016), improved light and extreme precipitation over the US (Li et al., 2012), and more realistic diurnal cycle of summertime convection over mid-latitude continents (Guichard et al., 2004; Khairoutdinov et al., 2005). Therefore, super-parameterized GCMs may be useful to provide guidance for improving sub-grid convective parameterizations. However, the additional computing cost for the super parameterization implementation is prohibitive for most modeling groups, which is a major reason why it is still not widely used.

In the analysis that follows we examine how models simulate deep tropical convective events, so it is worthwhile to summarize the behavior one might expect. Tropical convective clouds are often organized into a specific pattern known as the "building block model" (Mapes et al., 2006). Within this pattern, shallow convective clouds precede deep convective clouds which are then followed by stratiform anvil clouds. Shallow convective clouds pre-moisten the lower-troposphere and thus support the growth of deep convective clouds (Johnson et al., 1999; Sherwood, 1999; Sobel et al., 2004), while deep convective clouds detrain large amounts of condensate in the upper-troposphere and therefore contribute to the development of stratiform anvil clouds. The stratiform clouds, with cloud base near the melting level (Zipser, 1977), generate about 40 % of the tropical precipitation (Schumacher and Houze, 2003). Falling through the unsaturated air under the cloud base, some fraction of the stratiform precipitation evaporates, generating negatively buoyant downdrafts which may penetrate to the surface (Zipser, 1977). By mass continuity the stratiform downdrafts induce upward motion in the background atmosphere thus contributing to moistening and cooling of the lower-troposphere. The forced lift and the low-level moistening and cooling contribute to increasing low-level instability and thus may promote further initiation of new convection (Mapes, 1993; Mapes and Houze, 1995; Fovell et al., 2006). Some features of the building block models, the shallow convective pre-moistening and the strength of the stratiform circulation, have not been realistically simulated in global climate models (Mitovski et al., 2010).

For this study we use sub-hourly output from Version 4.3 of the Canadian Atmospheric Model (CanAM4.3) and version 5 of the super-parameterized Community Atmospheric Model (spCAM5) to isolate strong convective precipitation events in each model for a 3-month period in the Tropical Western Pacific (TWP). To evaluate the ability of CanAM4.3 to simulate convective precipitation relative to spCAM5 and the relationship between precipitation and the environment, composites of convective available potential energy (CAPE), CAPE generation in the free troposphere, large-scale near surface omega, and convective precipitation are analyzed for all convective events in this region.

2 Model description

Version 4.3 of the Canadian Atmospheric Global Climate Model (CanAM4.3) has several improvements relative to its predecessor, CanAM4 (von Salzen et al., 2013), including improvements to parameterizations of radiation and land surface processes. CanAM4.3 uses a hybrid vertical coordinate system with 49 levels between the surface and 1 hPa, with a resolution of about 100 m near the surface. The triangular spectral truncation of the model dynamical core is T63, with an approximate horizontal resolution of 2.8 degrees latitude/longitude.

The mass flux scheme of Zhang and McFarlane (ZM) is used in CanAM4.3 to parameterize the effect of deep convection on the large-scale environment (Zhang and McFarlane, 1995). The diagnostic closure of Zhang and McFarlane (1995) in CanAM4 has been replaced with a prognostic closure (Scinocca and McFarlane, 2004). The diagnostic closure assumes that convection consumes CAPE at a rate that is proportional to the (positive) difference between the ambient value and some specified threshold value. The triggering condition is that CAPE is greater than zero. A quasi-equilibrium state could emerge if the large-scale CAPE production balances the convective consumption but it is not imposed a-priori. The prognostic closure also does not assume quasi-equilibrium a-priori but a quasi-equilibrium state could in principle emerge. The trigger condition in the prognostic closure is also CAPE greater than zero. When activated, the prognostic closure computes the cloud base mass flux which increases proportionally with CAPE and is then dissipated within a specified time scale. To account for the effect of cumulus clouds with cloud tops below the ambient freezing level on the large-scale environment, CanAM4.3 employs a shallow convection scheme (von Salzen and McFarlane, 2002). The shallow convection scheme includes a parameterization of autoconversion processes to account for the effect of drizzle formation in shallow cumulus clouds following the approach in Lohmann and Roeckner (1996). The shallow convection scheme employs a diagnostic cloud base closure (Grant, 2001) based on a simplified turbulent kinetic energy budget for the convective boundary layer. The shallow scheme is not allowed to be active if the deep scheme is triggered at the same gridpoint and is vertically limited so that it operates mainly within the lower troposphere.

Version 5 of the Community Atmosphere Model (CAM5) used for the super-parameterized run has a horizontal resolution of 1.9° x 2.5° (latitude x longitude), ~~66 vertical levels from the surface to 5.1 x 10e-6 hPa~~ 30 vertical levels from the surface to 3.6 hPa, and a time step of 1800s for the physical parameterizations (Neale et al., 2012). Version 5.0 of the super-parameterized Community Atmosphere Model (spCAM5) employs a 2D CSRM within each CAM5 grid cell to replace the convective parameterization of moist convection and other atmospheric parameterizations. The CSRM uses 32 columns each with 4 km horizontal grid-spacing and 28 vertical layers, between 992 and 14.3 hPa, coinciding with the lowest 28 levels in CAM5. Details of the CSRM and information on CSRM implementation within CAM can be found in Khairoutdinov and Randall (2001 and 2003) and Wang et al., 2011.

For both models the period of analysis is limited to the period between May 1st and July 24th of 1997 after each model simulation has spun up (1 January 1996 to 30 April 1997 for CanAM4.3 and 1 January 1997 to 30 April 1997 for spCAM5). For CanAM4.3, a six member ensemble was generated by uniquely adjusting the seed for the random number generator on 1 January 1997. This was done to improve the statistical representation of the results from this model as data from all ensemble members were used in the analysis. The spCAM5 spin up is done using CAM5. Output over the domain 150°E – 170°E and 0°N – 10°N is extracted and used for our analysis. Over this domain the 4-km 10-minute CSRM output from spCAM5 is used to compute the quantities needed for the analysis while output from CanAM4.3 is available every 15 minutes (the model dynamical timestep). Both models used monthly varying prescribed SSTs and sea ice fractions based on observations (Hurrell et al., 2008) as well as transient concentrations of trace gases and aerosols that are representative of conditions during the time period of the simulations.

3 Methodology

3.1 Convective precipitation definition

Within spCAM5, the CAM5 atmospheric parameterizations ~~in CAM5~~ have been replaced by CSRMs, so it was necessary for our analysis to devise a method to separate the convective from the total precipitation. Convective precipitation in spCAM5 was defined to be the total precipitation from all convective CSRM columns divided by the total number of columns (i.e. divided by 32). Following the definition in Suhas and Zhang (2015) and Song and Zhang (2018), a CSRM column is categorized as convective if at any level the vertical velocity is greater than 1 m/s or less than -1 m/s and the sum of the cloud liquid and cloud ice water is greater than 0.1 g/kg. Convective precipitation in CanAM4.3 is generated within the deep and shallow convection schemes with the majority coming from the deep scheme.

The sensitivity of the results to the definition of convective precipitation from spCAM5 was evaluated by repeating the analyses using total instead of convective precipitation. The results in Figure 1, 2(a), 2(c), and 3 were found to be similar using either the total or convective precipitation from spCAM5, implying insensitivity, for this study, to the exact definition of thresholds in the method of Suhas and Zhang (2015).

3.2 Convective event definition

Previous studies used observations (Mapes et al., 2006; Mitovski et al., 2010) and cloud-resolving model simulations (Suhas and Zhang, 2015) to isolate strong precipitation events and diagnose convection-environment interactions relative to the peak of these events. Although this is a useful diagnostic approach for the development of closure schemes, it lacks information regarding initiation of precipitation. For our analysis, we use a slightly different approach. An initiation time (t_0) of a convective event is defined as the time at which convective precipitation within a GCM grid box exceeds 0.01 mm h^{-1} after following a 3-h period with no convective precipitation. An end time (t_f) of a convective event is defined as the time when convective precipitation, after exceeding 1 mm h^{-1}, drops down to less than 0.01 mm h^{-1} within a time period of up to 12 h after initiation. Using this approach, we isolated 831 convective events in spCAM5 and ~~328~~1452 in CanAM4.3 in the Tropical Western Pacific. Since the methodology isolates precipitating events that can last between 0.5 and 12 h, a scaled time (ST) is computed so that all events, regardless of lifetime, start and end at the same scaled time. The ST is calculated following Eq. (1):

$$ST(t) = \frac{(t - t_0)}{(t_f - t_0)} \times 100\ \% \qquad (1)$$

This approach improves comparison of composited events since features that precede or lag a rainfall peak, e.g. high CAPE and low convective inhibition (CIN) prior to peak rainfall and low CAPE and high CIN after peak rainfall, will occur at the same scaled time for all events regardless of lifetime.

3.3 Definition of convective available potential energy (CAPE) and CAPE generation

As defined in von Salzen and McFarlane (2002), CAPE, in J kg^{-1}, for an undiluted parcel of air rising from near the surface (SFC) to the level of neutral buoyancy (LNB) with the effect of condensate loading and without the effect of latent heat of fusion is calculated following Eq. (2):

$$CAPE = -g \int_{z_{SFC}}^{z_{LNB}} \frac{T_{vp} - T_{ve}}{T_{ve}}\, dz$$

(2)

where g is the gravity, T_{vp} is the virtual temperature of a rising air parcel, and T_{ve} is the virtual temperature of the large-scale environment.

CAPE as defined in Eq.2 includes two terms. The first term results from integration of the negative buoyancy between the surface and level of the free convection and represents the convective inhibition that the parcel of air has to overcome while it is lifted from the boundary layer into the convective layer. The second term results from integration over the region of positive buoyancy between the level of free convection and level of neutral buoyancy.

Following Zhang (2003, Eq. 5), CAPE is generated by radiative and advective large-scale processes $(\partial CAPE/\partial t)_{LS}$ and consumed by convective processes $(\partial CAPE/\partial t)_{CONV}$. The prognostic equation of CAPE is calculated following Eq. (3):

$$\frac{\partial CAPE}{\partial t} = \left(\frac{\partial CAPE}{\partial t}\right)_{LS} + \left(\frac{\partial CAPE}{\partial t}\right)_{CONV} \tag{3}$$

The large-scale (LS) generation term on the right hand side can be further separated into generation of CAPE by large-scale processes near the surface ($dCAPE_{LSS}$) and generation of CAPE by large-scale processes in the free troposphere ($dCAPE_{LSFT}$).

3.4 Definition of large-scale vertical velocity

By integrating the continuity equation in (x,y,p) coordinates, starting from the top of the atmosphere, ω (Pa s^{-1}) is computed from the mean divergence in a layer p using Eq. (4):

$$\omega_{p2} - \omega_{p1} = (p1 - p2)\left(\frac{\partial u}{\partial x} + \frac{\partial v}{\partial y}\right)_p \tag{4}$$

where omega at the top of the atmosphere is assumed to be zero, p1 is the pressure level above the layer p, and p2 is the pressure level under the layer p.

4. Results

4.1 Time-domain mean fields

Table 1 shows the domain (150°E – 170°E and 0°N – 10°N) and time (May – July) mean values for $dCAPE_{LSFT}$, ω, CAPE, and convective precipitation. Spatial standard deviations (in brackets) for each variable were computed using the time mean distributions over the domain. Both models show similar mean values for $dCAPE_{LSFT}$, ω, and convective precipitation. The CAPE values, however, are roughly 3-fold larger in spCAM5 (664 J kg^{-1}) than in CanAM4.3 (~~225~~220 J kg^{-1}). For comparison, we have computed CAPE using soundings from three tropical western Pacific sites: Truk/Caroline Is. (7.45º N and 151.8º E), Ponape/Caroline Is. (6.95º N and 158.2º E), and Majuro/Marshall Is. (7.08º N and 171.39º E). The observed May-July 1997 mean CAPE is 1080 J kg^{-1}.

The CAPE budget equation (Eq. 3) states that any change in CAPE between two time intervals is due to CAPE generation by the large-scale processes and due to CAPE consumption by convection during the two time intervals. It is known that in GCMs convection is activated too frequently (Zhang and Mu, 2005b) thus resulting in too frequent removal of CAPE and inability CAPE to accumulate to higher values. Since CanAM4.3 employs CAPE in its closure to compute mass flux and precipitation, too often activation will likely affect the precipitation rates resulting in too frequent too light precipitation. It

has been shown that GCMs tend to generate too frequent light precipitation (Sun et al., 2006; Dai, 2006; Wang et al. 2016) and underestimate the frequency of extreme precipitation (Wilcox and Donner, 2007; Boyle and Klein, 2010).

4.2 Frequency density of convective precipitation

Relative to spCAM5, CanAM4.3 overestimates the frequency of light convective precipitation (< 0.2 mm/h) and underestimates the frequency of extreme convective precipitation (> 2 mm h^{-1}) (Fig. 1b). Frequency density was defined as the ratio of the number of time steps with convective precipitation per 0.1 mm h^{-1} convective precipitation bin to the total number of time steps. When compared to observations, models also exhibit less rainfall variance (Sun et al., 2006; Dai, 2006; DeMott et al., 2007; Mitovski et al., 2010).

We show that $dCAPE_{LSFT}$ (Fig. 1a) increases with convective precipitation intensity in spCAM5 and in CanAM4.3. In addition, omega (ω) systematically increases with convective precipitation intensity in spCAM5 but not in CanAM4.3. For convective precipitation rates ~~>~~between ~~2~~0.5 and 2.5 mm h^{-1} CanAM4.3 shows a linear increase in ω ~~but the results are not considered robust due to the few samples (0.1 % corresponds to 8 samples per grid-cell) with these rates.~~

Convective events, as defined in Sect. 3.2, can last between 0.5 and 12 h. Figure 1c shows the fraction of convective events, from the total number of convective events, as a function of the event length. Figure 1d shows the average peak convective precipitation as a function of the event length. About 5 % of the 831 spCAM5 events last less than 1.5 h and 75 % of the events last between 1.5 and 3.0 h and only 1 % of the events last longer than 5 h (Fig. 1c) with the most intense convective precipitation being associated with longer lasting events (Fig, 1d). In comparison, 80 % of the ~~328~~1452 events in CanAM4.3 are shorter than 1.5 h and only 0.1 % of the events last longer than 5 h with the most intense convective precipitation being associated with shorter lasting events.

4.3 Relation between convective precipitation, large scale ω, and $dCAPE_{LSFT}$

In comparison to Figure 1a, which shows one quantity ($dCAPE_{LSFT}$ or ω) as a function of convective rainfall, Figure 2 shows convective rainfall histograms as function of two quantities. We find that convective precipitation in spCAM5 correlates best with both near surface -ω and $dCAPE_{LSFT}$ (Fig. 2a) with no dependence on CAPE (Fig. 2c). Reversible and undiluted CAPE computed from radiosonde profiles of temperature and humidity also shows that tropical precipitation intensity is not correlated with CAPE intensity (Mitovski and Folkins, 2014). As in Figure 1a, the strongest convective precipitation is associated with strong large-scale near surface ascent and strong $dCAPE_{LSFT}$. In addition, for a constant ω the rainfall rates increase with increasing $dCAPE_{LSFT}$ while for a constant value of $dCAPE_{LSFT}$ rainfall rates increase with decreasing ω (increasing ascent) with rain rates becoming more dependent on ω for larger $dCAPE_{LSFT}$. In the case when one of the quantities is in its lowest 25 percentile, for instance $dCAPE_{LSFT} \leq 50$ J kg^{-1} h^{-1} or $\omega > 80$ Pa s^{-1}, precipitation rates do not exceed 1 mm h^{-1}.

Precipitation simulated by CanAM4.3 (Fig. 2b) does not correlate with ω but does correlate with both CAPE and $dCAPE_{LSFT}$ (Fig. 2d) with greater rainfall rates being associated with larger values of CAPE and $dCAPE_{LSFT}$. This is expected since the precipitation generated within the ZM convection scheme is proportional to the updraft mass flux and the cloud water content. The updraft mass flux is closely related to the cloud base mass flux, which is computed within the prognostic CAPE based closure (Scinocca and McFarlane, 2004).

4.4 Composites over convective events

Prior the start of the convective event (time=0) in spCAM5 the near surface environment is characterized by a weak large-scale subsidence (Fig. 3a) and increasing relative humidity in the lower troposphere (Fig. 3g). An observed low-level moistening prior to deep convection has been previously attributed to moistening by shallow convective clouds (Sherwood, 1999; Sobel et al., 2004, DeMott et al., 2007). The moistening impacts the growth of convective clouds by modifying the dilution effect of entrainment on the buoyancy of rising air parcels (Sherwood, 1999; Raymond, 2000). The strength and depth of the pre-moistening are thus crucial in the transition from shallow to deep convection. The large-scale subsidence gradually weakens and diminishes about 20 min prior to time=0, roughly when CAPE reaches maximum and CIN reaches minimum (Fig. 3c). Therefore, a transition from a large-scale subsidence to large-scale ascent may be important in triggering convection. A near-surface omega tendency has been previously used as a trigger in the Donner convection scheme (Donner 1993; Wilcox and Donner 2007) in a version of the Geophysical Fluid Dynamic Laboratory (GFDL) Atmospheric model, version 3 (AM3) GCM. In their model, convection is triggered when near-surface omega becomes positive and exceeds a specified value and convective inhibition is less than 100 J kg-1. Although, $dCAPE_{LSFT}$ is positive prior to time=0 (Fig. 3e), precipitation is not initiated until ω becomes negative (large-scale ascent). The strongest ascent occurs around ST=45 %, shortly before the time of the strongest convective rainfall at ST=55 % and strongest $dCAPE_{LSFT}$ at ST=65 %. Although $dCAPE_{LSFT}$ shows great similarity with the convective precipitation, it lags the precipitation by ST=5-10 % which may imply that large-scale generation of $dCAPE_{LSFT}$ during the event life-time may be a consequence of the model dynamics, i.e. response of the model to convective heating. During the decaying phase, after ST=75 %, $dCAPE_{LSFT}$ is still relatively strong but ω becomes positive (subsidence), CAPE reaches minimum, and CIN reaches maximum , which likely prevent any further convection. Reversible and undiluted CAPE computed from 12-hourly radiosonde profiles of temperature and humidity shows similar behavior, with CAPE reaching a maximum prior to peak rainfall and minimum after peak rainfall (Mitovski and Folkins, 2014). The minimum CAPE and maximum CIN after peak rainfall are likely due to a combination of two effects, the export of boundary layer air with high moist static energy (MSE) into the middle troposphere by convective plumes and the injection of middle troposphere air with low MSE into the boundary layer by mesoscale downdrafts (Zipser, 1977; Sherwood and Wahrlich, 1999). The effect of these two processes will also contribute to low-level drying, which is seen in spCAM5, the low- to mid-level dip in the relative humidity patterns that occurs after peak rainfall, but not in CanAM4.3.

The large-scale environment prior the start of convective events in CanAM4.3 is quite different from spCAM5 with strong ascent and relatively weak CAPE. CanAM4.3 shows some moistening prior to time=0, but this moistening occurs in a very shallow layer near the surface leaving the troposphere between 900 and 600 hPa relatively dry. The shallow mass flux patterns (not included) indicate that shallow convection is only active in the lowest 100 hPa. Relative to observations, GCMs also tend to have drier lower troposphere which has been linked to convection schemes employed in the model (Wang and Zhang, 2013). Convective rainfall is found to occur once CAPE exceeds ~~360~~300 J/kg (Fig. 3d). In contrast to spCAM5, peak convective rainfall in CanAM4.3 (Fig. 3b) occurs closer to the end of the convective events corresponding with a peak in CAPE and CAPE generation (Fig. 3f). The strong correlation between convective precipitation and CAPE in CanAM4.3 is expected since convective precipitation in CanAM4.3 is proportional to cloud base mass flux which is in turn computed within the ZM prognostic closure as a function of CAPE (Scinocca and McFarlane, 2004). Convective precipitation in CanAM4.3 does not seem to correlate well with CIN (Fig. 3b) and this is likely because CIN is not independently included in the ZM closure in CanAM4.3. Therefore, any discussion of CIN and linkage to CanAM4.3

precipitation is out of the scope of this paper. We should point out thought that, CIN is tightly coupled with precipitation over mid-latitude summertime continent but not with precipitation over oceans (Myoung and Nielsen-Gammon, 2010).

The performance of various trigger functions and closures have been previously evaluated and it was found that in the tropics the best performing trigger functions are based on $dCAPE_{LSFT}$ and grid-scale vertical velocity in the lower troposphere (Suhas and Zhang, 2014; Song and Zhang, 2017). Replacing CAPE with $dCAPE_{LSFT}$ in the ZM closure resulted in the National Center for Atmospheric Research Community Climate Model, version 3 (NCAR CCM3), simulating a more realistic Madden-Julian Oscillation (Zhang and Mu, 2005a), improved summer and winter mean tropical precipitation and less frequent light precipitation (Zhang and Mu, 2005b). Including a relative humidity at the parcel origin in the trigger function also improves the simulation of convection (Zhang and Mu, 2005b; Suhas and Zhang, 2014).

In general, most commonly used deep convection schemes in climate models employ closures based on CAPE or based on net column moisture convergence. We show that convective precipitation generated within a CAPE based closure is correlated to CAPE and CAPE generation in the free troposphere, while in spCAM5 precipitation is correlated to $dCAPE_{LSFT}$ and ω. Since we computed ω from the horizontal winds starting from the top of the atmosphere (Eq. 4), near surface ω is closely linked with the net column mass convergence. Thus, it would be beneficial to compare correlation of convective precipitation generated within a net column moisture convergence based closure.

5. Summary

In the absence of high spatial resolution and sub-hourly observations, sub-hourly output from a super-parameterized AGCM (spCAM5) was used to study interactions between convective precipitation and the large-scale environment in the tropical western Pacific and to evaluate these interactions in a traditional AGCM (CanAM4.3). This is done by compositing model output of CAPE, CAPE generation in the free troposphere ($dCAPE_{LSFT}$), and large-scale near surface vertical velocity (ω) over convective events during 1 May and 24 July 1997.

Although the domain mean convective precipitation, $dCAPE_{LSFT}$, and ω are found to be similar in the simulation period of May – July 1997 (Table 1), notable differences between CanAM4.3 and spCAM5 are found when compositing over convective events. The lengths of the convective events are shorter in CanAM4.3 with 80 % of the events lasting less than 1.5 h compared to 5 % in spCAM5. The strongest convective precipitation in CanAM4.3 is generated within shorter events while the strongest convective precipitation in spCAM5 is associated with longer lasting events. Compared to spCAM5, CanAM4.3 overestimates the frequency of light convective precipitation (< 0.2 mm h^{-1}) and underestimates the frequency of extreme convective precipitation (> 2 mm h^{-1}). When evaluated against observations, GCMs also tend to produce too frequent too light precipitation (Sun et al., 2006; Dai, 2006; Wang et al. 2016) which has been related to too frequent activation of CAPE based convective scheme (Zhang and Mu, 2005b).

Interaction with the large-scale environment is found to differ between the models. In spCAM5, the maximum relative humidity is in the boundary layer roughly 1 h prior to t=0 (Fig. 3g). Increasing boundary layer moistening prior to peak rainfall seen in observations has been attributed to pre-moistening by shallow convective clouds prior to deep convection (Johnson et al., 1999; Sherwood, 1999; Sobel et al., 2004). The large-scale subsidence changes to large-scale ascent prior to t=0, and is coincident with the maximum CAPE value. After the initiation time in spCAM5, there is similarity between variations in ω , $dCAPE_{LSFT}$, and convective precipitation, with variations in omega slightly preceding and variations in $dCAPE_{LSFT}$ slightly lagging variations in convective precipitation. In CanAM4.3 no dependence on ω was found, instead the model shows a dependence on CAPE and $dCAPE_{LSFT}$. The spCAM5 relative humidity patterns show a “dip” after peak

rainfall, which has been previously linked to the injection of low moist static energy air from the middle into lower troposphere by mesoscale downdrafts (Zipser, 1977; Sherwood and Wahrlich, 1999). Although the relative humidity in CanAM4.3 has maximum in the boundary layer, this maximum is more persistent about peak rainfall and it occurs in a thin layer close to the surface. The height and time of the maximum humidity is coincident with the height and time of the shallow convective mass flux, suggesting that shallow convection, although important in moistening the boundary layer, does not penetrate to higher levels leaving the troposphere above 900 hPa relatively dry.

Although the sub-grid moist convection is a very complicated topic, in this study we see evidence that precipitation variability can be influenced by the design and the nature of the trigger and closure functions. The diagnostics described in this paper provide information regarding initiation and evolution of rainfall and can be used to study trigger conditions necessary for initiation of deep convection and the deep convection closure in regional and global models. We thus suggest that it is worthwhile to investigate the sensitivity of the precipitation generated within the ZM scheme in CanAM4.3 to various trigger and closure assumptions.

Code and data availability: Codes to perform the analysis described in the manuscript are available at https://github.com/jc-cccma/sub-hourly-convection-analysis with version 32.0.0 having the ~~DOI~~ DOI: 10.5281/zenodo.2560671 ~~https://doi.org/10.5281/zenodo.1442382~~. Model output from spCAM5 and CanAM4.3 that are to be used as input for the codes can be found at ftp://ftp.cccma.ec.gc.ca/pub/jcole/GMD_MITOVKSI_2018/DATA.

Author contributions: TM conceived the method, performed the analysis and wrote the manuscript, JC designed and performed the CanAM4.3 simulations as well as contributing to writing the manuscript. KS and NM provided expert advice to improve the analysis and the manuscript. GJZ supplied spCAM5 model output and provided advice to improve the analysis.

Acknowledgments: The authors are grateful to Dr. Paul Vaillancourt and Dr. Rashed Mahmood for reviewing the manuscript. The authors also thank Chengzhu (Jill) Zhang of Lawrence Livermore National Laboratory for providing the spCAM5 output used in this study.

GJZ is supported by the U.S. Department of Energy, Office of Science, Biological and Environmental Research Program (BER), under Award Number DE-SC0016504.

References:

Arakawa, A., and Schubert, W. H.: Interaction of a cumulus cloud ensemble with the large-scale environment, Part 1, J. Atmos. Sci., 31(3), 674–701, 1974.

Bechtold, P., Bazile, E., Guichard, F., Mascart, P.,, and Richard, E.: A mass-flux convection scheme for regional and global models, Q. J. R. Meteorol. Soc., 127(573), 869–886, 2001.

Bechtold, P., Semane, N.,, Lopez, P.,, Chaboureau, J.,, Beljaars, A.,, and Bormann, N.: Representing Equilibrium and Nonequilibrium Convection in Large-Scale Models. J. Atmos. Sci., 71, 734–753, https://doi.org/10.1175/JAS-D-13-0163.1, 2014.

Boyle, J., and Klein, S. A.: Impact of horizontal resolution on climate model forecasts of tropical precipitation and diabatic heating for the TWP-ICE period, J. Geophys. Res., 115, D23113, doi:10.1029/2010JD014262, 2010.

Dai, A.: Precipitation characteristics in eighteen coupled climate models. J. Climate, 19, 4605 4630, doi:10.1175/JCLI3884.1, 2006

DeMott, C., Randall, D. A., and Khairoutdinov, M.: Convective precipitation variability as a tool for general circulation model analysis, J. Climate, 20, 91-112, doi:10.1175/JCLI3991.1, 2007.

Done, J. M., Craig, G. C., Gray, S. L., Clark, P. A., and Gray, M. E. B.: Mesoscale simulations of organized convection: Importance of convective equilibrium, Q. J. R. Meteorol. Soc., 132: 737–756, doi:10.1256/qj.04.84, 2006.

Donner, L. J.: A cumulus parameterization including mass fluxes, vertical momentum dynamics, and mesoscale effects. J. Atmos. Sci., 50, 889–906, doi:10.1175/1520-0469(1993)050,0889: ACPIMF.2.0.CO;2, 1993.

Fovell, R. G., Mullendore, G., and Kim, S. H.: Discrete propagation in numerically simulated nocturnal squall lines, Mon. Wea. Rev., 134, 3735 – 3752, 2006.

Grabowski, W.W.: Coupling cloud processes with the large-scale dynamics using the cloud-resolving convection parameterization (CRCP). J. Atmos. Sci., 58, 978–997, https://doi.org/10.1175/1520-0469(2001)058<0978:CCPWTL>2.0.CO;2, 2001.

Grant, A. L. M.: Cloud-base fluxes in the cumulus-capped boundary layer, Q. J. R. Meteorol. Soc., 127:407–421, 2001.

Guichard, F., Petch, J. C., Redelsperger, J.-L., Bechtold, P., Chaboureau, J.-P., Cheinet, S., Grabowski, W., Grenier, H., Jones, C. G., Köhler, M., Piriou, J.-M., Tailleux, R. and Tomasini, M.: Modelling the diurnal cycle of deep precipitating convection over land with cloud-resolving models and single-column models. Q.J.R. Meteorol. Soc., 130: 3139–3172. doi:10.1256/qj.03.145, 2004.

Hurrell, J.W., Hack, J. J., Shea, D., Caron, J. M., and Rosinski, J.: A new sea surface temperature and sea ice boundary dataset for the community atmosphere model. J. Climate, 21, 5145–5153, https://doi.org/10.1175/2008JCLI2292.1, 2008.

Johnson, R.H., Rickenbach, T. M., Rutledge, S. A., Ciesielski, P. E., and Schubert, W. H.: Trimodal characteristics of tropical convection. J. Climate, 12, 2397-2418, 1999.

Khairoutdinov, M. F. and Randall, D. A.: A cloud resolving model as a cloud parameterization in the NCAR community climate system model: preliminary results. Geophys, Res. Lett., 28: 3617–3620, 2001.

Khairoutdinov, M. F. and Randall, D. A.: Cloud resolving modeling of the ARM summer 1997 IOP: Model formulation, results, uncertainties, and sensitivities, J. Atmos. Sci., 60, 607–625, 2003.

Khairoutdinov, M. F., Randall, D. A., and DeMott, C.: Simulations of the atmospheric general circulation using a cloud resolving model as a super-parameterization of physical processes,J. Atmos. Sci., 62, 2136–2154, doi:10.1175/JAS3453.1, 2005.

Kooperman, G. J., Pritchard, M. S., Burt, M. A., Branson, M. D., and Randall, D. A.: Robust effects of cloud superparameterization on simulated daily rainfall intensity statistics across multiple versions of the Community Earth System Model, J. Adv. Model. Earth Syst., 8, 140–165, doi:10.1002/2015MS000574, 2016.

Li, F., Rosa, D., Collins W. D., and Wehner, M. F.: ‘‘Super-parameterization’’: A better way to simulate regional extreme precipitation?, J. Adv. Model. Earth Syst., 4, M04002, doi:10.1029/2011MS000106, 2012.

Lohmann U., and Roeckner, E.: Design and performance of a new cloud microphysics scheme developed for the ECHAM general circulation model, Clim. Dyn., 12:557–572, 1996.

Mapes, B. E.: Gregarious tropical convection, J. Atmos. Sci., 50, 2026 – 2037, 1993.

Mapes, B. E., and Houze, Jr., R. A.: Diabatic divergence profiles in tropical mesoscale convective systems, J. Atmos. Sci., 52, 1807-1828, 1995.

Mapes, B., Tulich, S., Lin, J., and Zuidema, P.: The mesoscale convection life cycle: Building block or prototype for large-scale tropical waves?. Dynamics of Atmospheres and Oceans, 42. 3-29. 10.1016/j.dynatmoce.2006.03.003, 2006.

Mauritsen, T., et al.: Tuning the climate of a global model, J. Adv. Model. Earth Syst., 4, M00A01, doi:10.1029/2012MS000154, 2012.

Mitovski, T., Folkins, I., von Salzen, K., and Sigmond, M.: Temperature, relative humidity, and divergence response to high rainfall events in the tropics: Observations and models, J. Clim., 23, 3613-3625, doi:10.1175/2010JCLI3436.1, 2010.

Mitovski, T., and Folkins, I.: Anomaly patterns about strong convective events in the tropics and midlatitudes: Observations from radiosondes and surface weather stations, J. Geophys. Res. Atmos., 119, 2014.

Myoung, B. and Nielsen-Gammon J. W.: Sensitivity of Monthly Convective Precipitation to Environmental Conditions. J. Climate, **23**, 166–188, https://doi.org/10.1175/2009JCLI2792.1, 2010.

Neale, R. B., and Coauthors.: Description of the NCAR Community Atmosphere Model (CAM 5.0). NCAR Tech. Note TN-486, 274 pp, 2012.

Raymond, D.: Thermodynamic control of tropical rainfall. Q. J. R. Meteorol. Soc., 126, 889–898, 2000.

Schumacher, C., and Houze Jr., R. A.: Stratiform rain in the tropics as seen by the TRMM Precipitation Radar. J. Climate, 16, 1739-1756, 2003.

Scinocca, J. F., and McFarlane, N. A.: The variability of modeled tropical precipitation. J. Atmos. Sci., 61, 1993–2015, 2004.

Sherwood, S. C.: Convective precursors and predictability in the tropical western Pacific, Mon. Wea. Rev., 127, 2977-2991, 1999.

Sherwood, S. C., and Wahrlich, R.: Observed evolution of tropical deep convective events and their environment. Mon. Wea. Rev., 127, 1777-1795, 1999.

Sobel, A. H., Yuter, S. E., Bretherton, C. S., and Kiladis, G. N. : Large-scale meteorology and deep convection during TRMM KWAJEX. Mon. Wea. Rev., 132, 422–444, 2004.

Song, F., and Zhang, G. J.: Improving trigger functions for convective parameterization schemes using GOAmazon observations. *J. Climate*, **30**, 8711-8726, DOI: 10.1175/JCLI-D-17-0042.1, 2017.

Song, F., and Zhang, G. J.: Understanding and Improving the Scale Dependence of Trigger Functions for Convective Parameterization Using Cloud-Resolving Model Data. J. Climate, **31**, 7385–7399, https://doi.org/10.1175/JCLI-D-17-0660.1, 2018.

Stan, C., Khairoutdinov, M., DeMott, C. A., Krishnamurthy, V., Straus, D. M., Randall, D. A., Kinter III, J. L., and Shukla, J.: An ocean-atmosphere climate simulation with an embedded cloud resolving model, Geophys. Res. Lett., 37, L01702, doi:10.1029/2009GL040822, 2010.

Suhas, E. and Zhang, G. J.: Evaluation of trigger functions for convective parameterization chemes using observations. J. Climate, 27, 7647–7666, https://doi.org/10.1175/JCLI-D-13-00718.1, 2014.

Suhas, E., and Zhang, G. J.: Evaluating convective parameterization closures using cloud resolving model simulation of tropical deep convection, J. Geophys. Res. Atmos., 120, doi:10.1002/2014JD022246, 2015.

Sun, Y., Solomon, S., Dai, A., and Portmann, R.: How often does it rain? J. Climate, 19, 916–934, 2006.

Thayer-Calder, K., and Randall, D. A.: The role of convective moistening in the Madden-Julian Oscillation. J. Atmos. Sci., 66, 3297–3312, https://doi.org/10.1175/2009JAS3081.1, 2009.

Tiedtke, M.: A comprehensive mass flux scheme for cumulus parameterization in large-scale models, Mon. Wea. Rev., 117, 1779–1800, 1989.

Truong, N. M., Tien, T. T., Pielke Sr., R. A., Castro, C. L., and Leoncini, G.: A modified Kain–Fritsch scheme and its application for simulation of an extreme precipitation event in Vietnam. Mon. Wea. Rev., 137, 766–789, doi:10.1175/2008MWR2434.1, 2009.

Varble, A., Fridlind, A. M., Zipser, E. J., Ackerman, A. S., Chaboureau, J. -P., Fan, J., Hill, A., McFarlane, S. A., Pinty, J. -P., and Shipway, B.:Evaluation of cloud-resolving model intercomparison simulations using TWP-ICE observations: Precipitation and cloud structure, J. Geophys. Res., 116, D12206, doi:10.1029/2010JD015180, 2011.

von Salzen, K. and McFarlane, N. A.: Parameterization of the bulk effects of lateral and cloud-top entrainment in transient shallow cumulus clouds. J. Atmos. Sci., 59, 1405–1430, https://doi.org/10.1175/1520-0469(2002)059<1405:POTBEO>2.0.CO;2, 2002.

von Salzen, K., Scinocca, J. F., McFarlane, N. A., Li, J., Cole, J. N. S., Plummer, D., Verseghy, D., Reader, M. C., Ma, X., Lazare, M., and Solheim, L.: The Canadian Fourth Generation Atmospheric Global Climate Model (CanAM4). Part I: representation of physical processes. Atmosphere-Ocean, 51, 104-125, doi:10.1080/07055900.2012.755610, 2013.

Wang, M., Ghan, S., Easter, R., Ovchinnikov, M., Liu, X., Kassianov, E., Qian, Y., Gustafson Jr., W. I., Larson, V. E., Schanen, D. P., Khairoutdinov, M., and Morrison, H.: The multi-scale aerosol-climate model PNNL-MMF: model description and evaluation, Geosci. Model Dev., 4, 137-168, https://doi.org/10.5194/gmd-4-137-2011, 2011.

Wang, X., and Zhang, M.: An analysis of parameterization interactions and sensitivity of single-column model simulations to convection schemes in CAM4 and CAM5, J. Geophys. Res. Atmos., 118, 8869–8880, doi:10.1002/jgrd.50690, 2013.

Wang, Y., Zhang, G. J., and Craig, G.: Stochastic convective parameterization improving the simulation of tropical precipitation variability in the NCAR CAM5, Geophys. Res. Lett., 43, doi:10.1002/2016GL069818, 2016.

Wang, Y., Zhang, G. J., and He, Y. J.: Simulation of precipitation extremes using a stochastic convective parameterization in the NCAR CAM5 under different resolutions, J. Geophys. Res.-Atmospheres, 122, https://doi.org/10.1002/2017JD026901, 2017.

Wilcox, E.M. and Donner, L. J.: The Frequency of Extreme Rain Events in Satellite Rain-Rate Estimates and an Atmospheric General Circulation Model. J. Climate, 20, 53–69, https://doi.org/10.1175/JCLI3987.1, 2007.

Zhang, G. J.:Convective quasi-equilibrium in the tropical western Pacific: Comparison with midlatitude continental environment, J. Geophys. Res., 108(D19), 4592, doi:10.1029/2003JD003520, 2003.

Zhang, G. J., and McFarlane, N. A.: Sensitivity of climate simulations to the parameterization of cumulus convection in the CCC-GCM. Atmos.–Ocean, 3, 407–446, 1995.

Zhang, G. J. and Mu, M.: Simulation of the Madden-Julian Oscillation in the NCAR CCM3 Using a Revised Zhang-McFarlane Convection Parameterization Scheme. J. Climate, 18, 4046–4064, https://doi.org/10.1175/JCLI3508.1, 2005a.

Zhang, G. J. and Mu, M.: Effects of modifications to the Zhang-McFarlane convection parameterization on the simulation of the tropical precipitation in the National Center for Atmospheric Research Community Climate Model, version 3, J. Geophys. Res., 110, D09109, doi:10.1029/2004JD005617, 2005b.

Zipser, E. J.: Mesoscale and convective-scale downdrafts as distinct components of a squall-line structure. Mon. Wea. Rev., 105, 1568 – 1589, 1977.

Table 1

Variable	SpCAM5	CanAM4.3
	MEAN (St. Dev)	MEAN (St. Dev)
$dCAPE_{LSFT}$ (J/kg/h)	52 (19)	~~54~~50 (~~10~~13)
ω (Pa/h)	-16 (6)	-~~12~~8 (~~12~~10)
CAPE (J/kg)	664 (94)	~~225~~220 (~~57~~67)
Convective prec. (mm/h)	0.28 (0.10)	0.~~27~~28 (0.0~~4~~6)

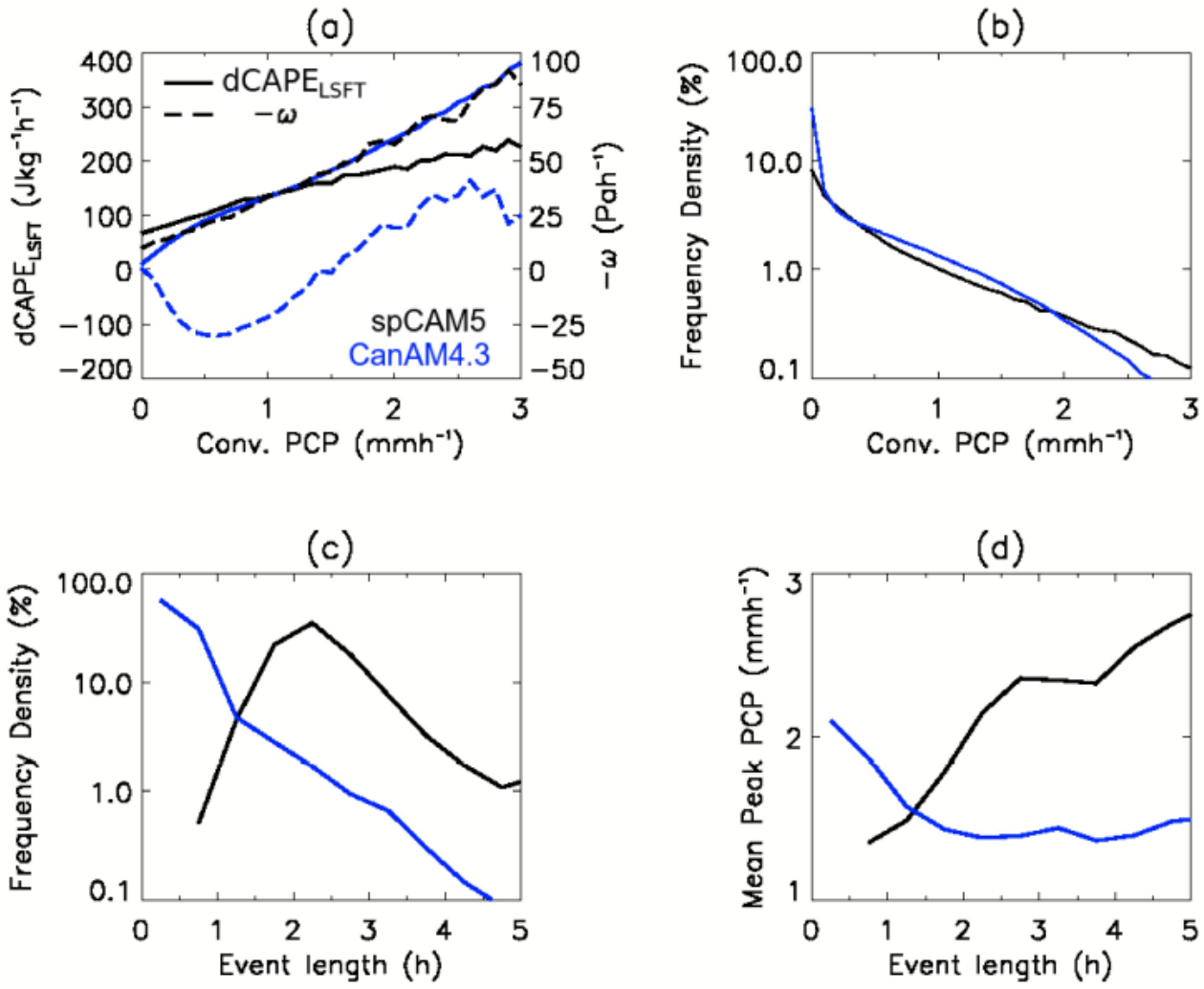

Figure 1: (a) Mean values of CAPE generation in the free troposphere (solid) and near surface large-scale -ω (dashed) per 0.1 mm/h convective precipitation bin in spCAM5 (black) and CanAM4.3 (blue), (b) frequency density of convective precipitation per 0.1 mm/h bin. Frequency density of 1 % in (b), or 1 mm/h convective precipitation in (a) and (b), corresponds to 82 CanAM4.3 and 122 spCAM5 samples per grid-cell. (c) frequency density of convective event length, (d) mean peak convective precipitation as function of convective event length. Frequency density of 10 % in (c) corresponds to 33 CanAM4.3 and 83 spCAM5 convective events.

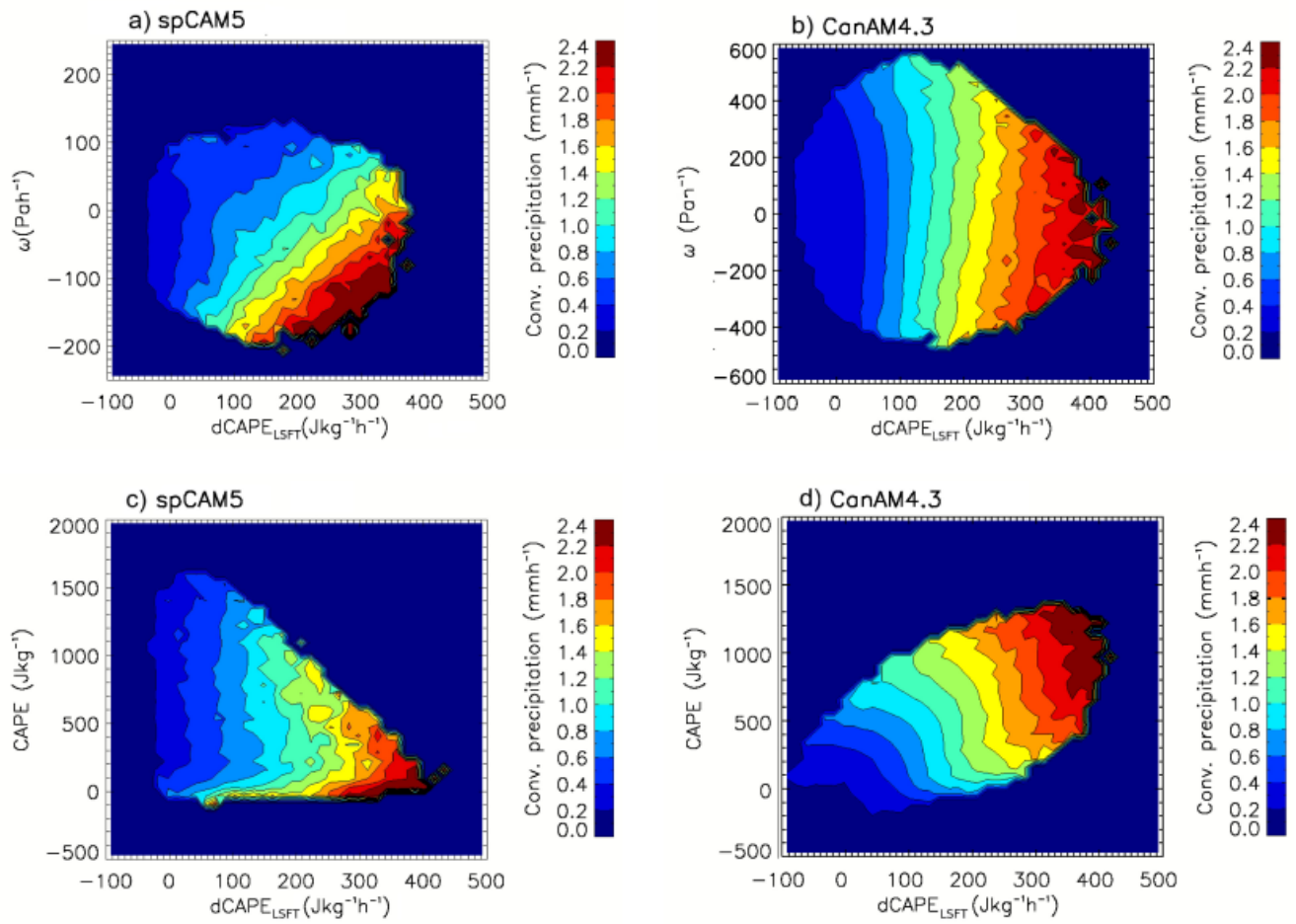

Figure 2: (a) spCAM5 and (b) CanAM4.3 mean convective precipitation as function of near surface ω and $dCAPE_{LSFT}$. (c) spCAM5 and (d) CanAM4.3 mean convective precipitation as function of CAPE and $dCAPE_{LSFT}$. Each of the plots consists of 1600 bins, 40 on X-axis and 40 on Y-axis. The convective precipitation within each bin is an average of at least 20 values.

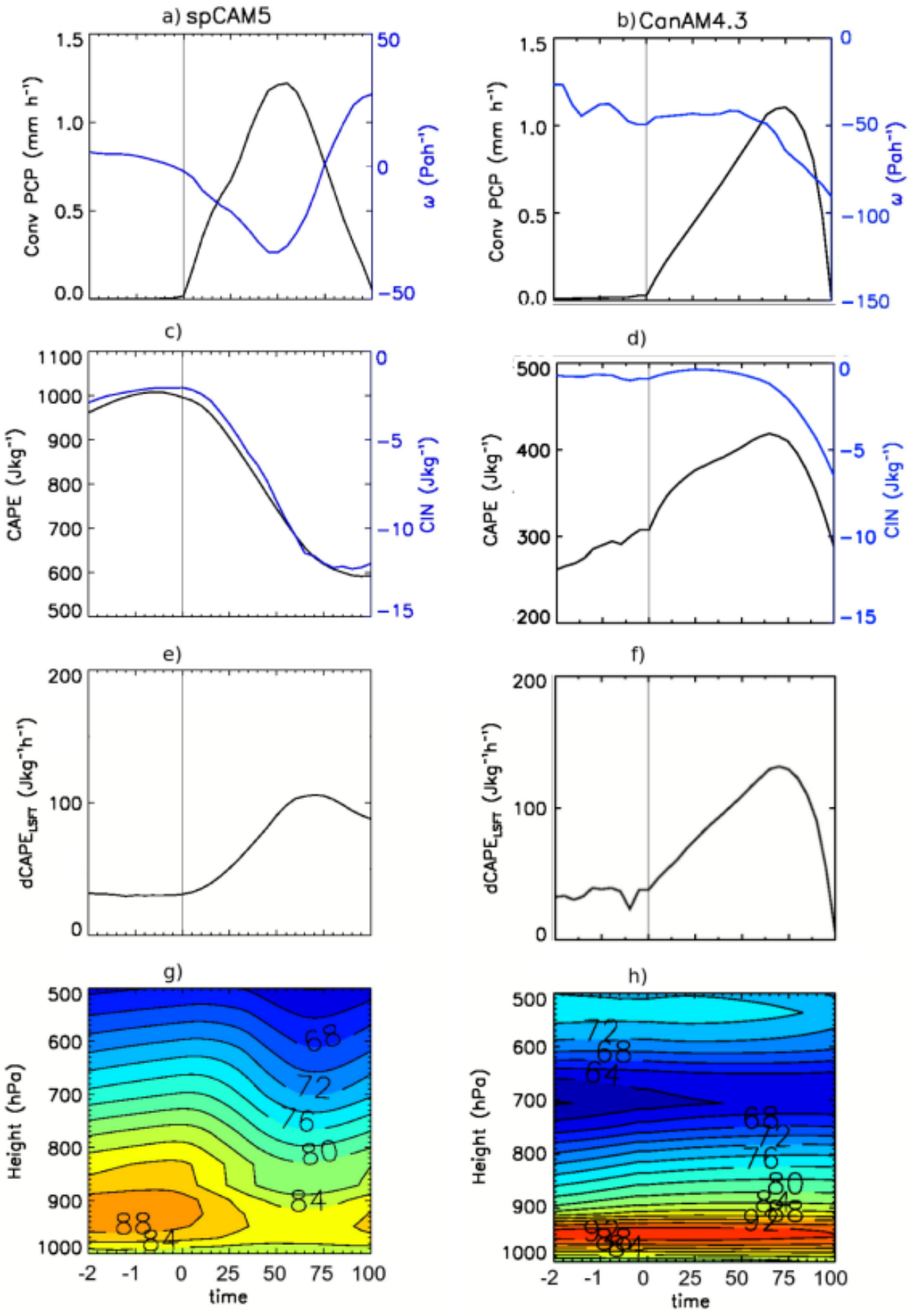
a) spCAM5
b) CanAM4.3
Conv PCP (mm h⁻¹)
ω (Pah⁻¹)
c)
d)
CAPE (Jkg⁻¹)
CIN (Jkg⁻¹)
e)
f)
dCAPE_LSFT (Jkg⁻¹h⁻¹)
g)
h)
Height (hPa)
time

Figure 3: Prior to time=0, the time on the x-axis is in hours. After time=0, the time is in % of the event duration time. The rain events start at time=0 and end at t=100. The y-axis on the left shows values for the black curves and the y-axis on the right shows values for the blue curves. The panels on the left are for spCAM5 and the panels on the right are for CanAM4.3. The first row shows convective precipitation and large-scale near surface ω; the second row shows CAPE and CIN; the third row shows $dCAPE_{LSFT}$, and the fourth row show relative humidity patterns.